Research Article

Human hair follicle biomagnetism: potential biochemical correlates

Abraham A. Embi[1] and Benjamin J. Scherlag[2]

[1] 13442 SW 102 Lane Miami, FLA, 33186, USA
[2] Heart Rhythm Institute, University of Oklahoma Health Sciences Center, Oklahoma City, Oklahoma, USA

Received on May 21, 2015; Accepted on June 29, 2015; Published on July 18, 2015

Correspondence should be addressed to Abraham A. Embi; Tel: +1 305 387 6102, E-mail: embi21@att.net

Abstract

Background: The S100 protein family is linked to energy transfer in cells of vertebrates at a molecular level. This process involves the electron transfer chain and therefore, as inferred from Faraday's Law, electron movement will induce electromagnetic fields (EMFs). Biological entities emit photoelectrons that can be tracked and visualized by small paramagnetic nano-sized iron particles.
Methods: We have developed an optical microscopic approach for imaging electromagnetic activity of hair follicles utilizing nano-sized iron particles (mean diameter 2000nm) in Prussian Blue Stain solution (PBS Fe 2000).
Results: We found that the human hair follicle emits electromagnetic fields (EMFs) based on metabolic activity within the follicle, which is associated with the activity of selective S-100 proteins.
Conclusions: Our results link the molecular biochemical energy associated with the S100 family of proteins and biomagnetism of human hair follicles.

Introduction

In the first report of EMF measurements made from the human heart, Baule & McFee (1963) used two large coils placed over the chest to cancel ambient magnetic interference. Better resolution and less noise was later achieved by Cohen and his associates who recorded EMFs from the brain (Cohen 1972) and the heart (Cohen & Kaufman 1975, Cohen *et al.* 1983) using a superconducting quantum interference device (SQUID). We hypothesize that all living matter maintains an intrinsic, electromagnetic homeostatic mechanism at quantum levels, based on biochemical and biophysical processes. From sub-atomic and atomic interactions, there are ordered amplifications manifesting as metabolic activity to maintain homeostasis. Photon-phonon and photon-photon transductions, i.e. piezoelectricity and photoelectricty may be underlying mechanisms to explain bio-electromagnetic order and balanced function in living things. Utilizing the intrinsic paramagnetic properties of fine iron particles, and the imaging characteristics of iron by Prussian Blue stain, a solution was developed which could be applied to human hairs *ex vivo*. Magnetic energy was detected and visualized by the stained, aggregated iron particles applied to the follicle and shaft of human hairs. Since some of the S100 family of proteins involved in energy exchanges have been localized in anatomically discreet areas of the human hair follicle (Mitoma *et al.* 2014), we proceeded to attempt a correlation between such

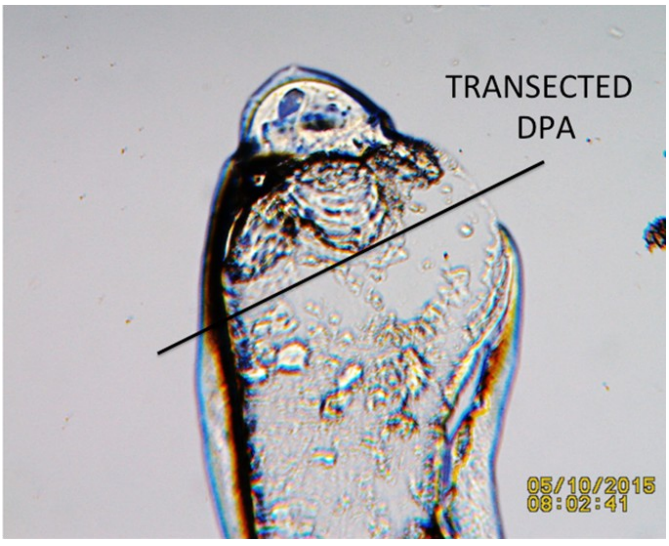

Figure 1. Microphotograph (x14 magnification) showing sebum imprint of human hair follicle (bulb area), depicting the dermal papilla area (DPA). The transected area is shown above the straight line, similarly to Figure 3. The plucked human hair is covered by sebum that is left behind after the hair is removed.

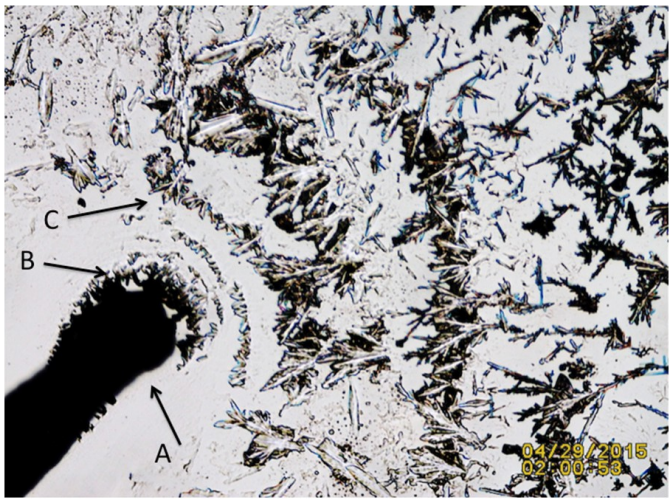

Figure 2. Microphotograph (X10 magnification) of a SSP of PBSFe2000 of human hair dry field. Living matter (hair follicle) is seen triggering crystallization. A depicts the hair bulb; B depicts the crystals adhering to the DP area and C depicts the layered crystallization. Please note that the KFeCN crystals triggered by the EMFs remain in front of the hair follicle which is the putative S100, S4, S6 localization (see Supplementary Video 2).

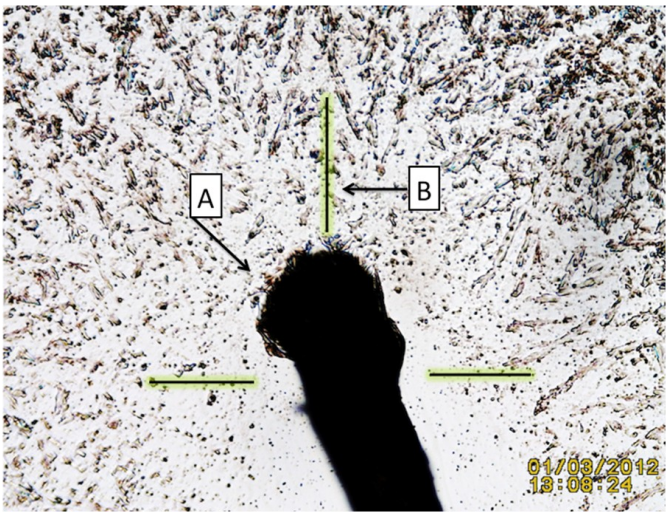

Figure 3. SSP PBSFe2000 after evaporation. Microphotohraph (x10 magnification) showing the human hair follicle post-blade excision of the DP area. Notice the absence of heavy crystallization in front of the hair (facing the evaporation line). This absence correlates with the lack of EMFs strong enough to trigger heavy crystallization. This finding is attributed to the removal of the DP as illustrated in Figure 1.

areas; specifically, the follicular tissue and electromagnetic activity.

Materials and Methods

Preparation of the iron containing solution

A fine iron particle solution was prepared by mixing several grams of powdered iron filings (Edmond Scientific Co., Tonawanda, NY) in 200 cc of deionized water (resistivity, 18.2 MΩ.cm). After standing for several hours the supernatant was carefully decanted for sizing of the iron nano-sized iron particles. The particle size and distribution of the nanoparticles from the supernatant was determined using dynamic light scattering (DLS) and the zeta potential using phase analysis light scattering by a Zeta potential analyzer (ZetaPALS, Brookhaven Instruments Corp, Holtsville, NY). For sizing, 1.5 ml of the solution in de-ionized water was scanned at 25 °C and the values were obtained in nanometers (nm). A similar aliquot of the fine iron particle solution was scanned for 25 runs at 25 °C. for determining zeta potentials. Zeta potential values were displayed as millivolts (mV). Using a transfer pipette, aliquots of the solution containing the iron particles (with a mean particle size of 2000 nm) were combined with Prussian Blue Stain (PBS, 2.5% potassium Ferrocyanide and 2.5% hydrochloric acid).

The single slide preparation (SSP)

Hairs (n = 4) in the Telogen phase were individually placed on a clean slide (size 25 x 75 x1mm). The freshly plucked human hairs (from the author's scalp) were positioned in the center of the slide. This was facilitated by the inherent stickiness of the hair root. Three drops of the PBSFe2000 solution were placed in the center of the aforementioned clean glass microscopic slide. Care was also taken to cover the root and shaft area and then the liquid was allowed to evaporate. The viewing and event recordings of the evaporation (still pictures or videos) of the slides were done in the normal mode at X10 magnification with a video microscope (Celestron LCD Digital Microscope II model #4341; Torrance ,California, USA).

Transected Hair follicles

Hairs were placed on a clean slide (size 25 x 75 x 1mm). The freshly plucked *ex vivo* hairs were individually positioned in the center of the slides. At this point with the aid of a magnifying glass and a razor blade, the hair follicle was transected at approximately the distal part of the root (Figure 1).

Upon viewing in the microscope (X10 magnification), the transections that did not satisfy our criteria (n=13) of separating the distal bulb from the follicle were discarded. Four samples (successfully transected) (n = 4) were studied by applying 3 drops of the PBSFe2000 solution over the follicle and shaft, mounted on a clean slide and then the liquid was allowed to evaporate. The viewing and event recordings of the evaporation were handled similarly in a series of controls (n = 2), using a non-animate source of EMF (see ancillary experiments in the Results section).

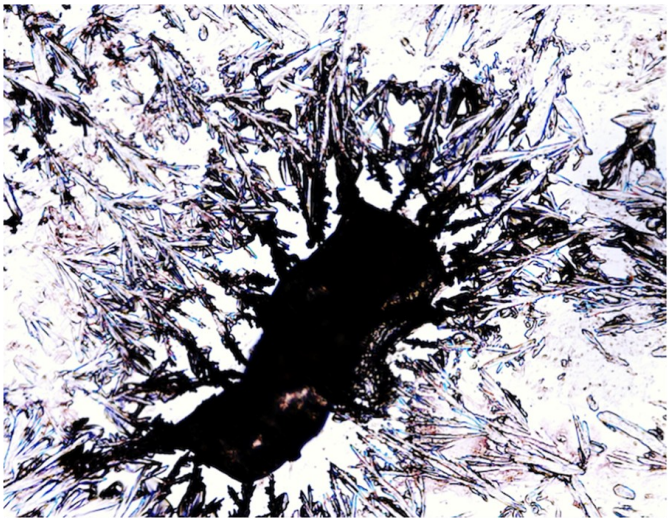

Figure 4. SSP of PBSFe2000 dry field. Microphotograph (x14 magnification) of excised tissue from the human hair follicle shown in Figure 1. Anatomically, this tissue corresponds to the DP area. Notice the heavy crystals attracted to the tissue surface is attributed to the maintenance of metabolism with the presence of S100 proteins and associated EMFs.

Results

In the wet field of the follicles mounted in a SSP, we consistently noticed iron particles circulating around the distal part of the hair follicle (bulb) (n = 4), similarly to our previous findings (Embi *et al.* 2015a, b). The circulating iron particles were interpreted as the presence of EMFs emanating from the hair root. In the dry field after evaporation all control hairs showed layered crystallization of the PBSFe2000. These layers correlated with the EMFs emitted by the follicle. Anatomical areas of the hair such as the hair shaft covered by cuticles expressed weak S100 A2 as well as showing the absence of layered crystallization. In contrast, the distal root area where the dermal papilla (DP) is located has been shown to express S100 A4 and S100 A6 proteins (Mitoma *et al.* 2014). In all our experiments this area consistently triggered heavy concentration of layered crystallization directly adherent to the bulb as seen in Figure 2.

In other experiments, the hair follicle was cut or transected proximal to the DP, thereby separating the DP from the rest of the follicle. When subjected to the same SSP procedures, the rest of the cut follicle (minus the DP) exhibited no crystals adhering to its surface (Figure 3). On the other hand, the isolated DP tissue fragment showed a clear intense crystallization pattern, which adhered to its surface (Figure 4).

Ancillary Experiments

Inanimate magnetized material

When a non-living entity such as a magnet fragment which is absent of any S100 proteins, was cut to a similar size of a hair follicle and placed in a SSP with PBSFe200, layered crystallization ensued (n = 2). There were no crystals which adhered to the part of the magnet first encountering the evaporation line, which, by its location in this model mimics the excised DP. This ancillary experiment served as a control since non-animate EMFs from the magnet trigger an orderly display of crystallization lines, stopping short of touching the magnetic fragment itself. (Figure 5 and Supplementary Video 1)

Inanimate nonmagnetic material

When a non-living entity such as a dead wood fragment which is absent of any S100 proteins, was cut to a similar size of a hair follicle and placed in a SSP with PBSFe200, layered crystallization failed to ensue. This ancillary experiment served as a negative control. The absence of EMFs is attributed to the failed crystallization. See Figure 6 below and Supplementary Video 2.

Discussion

Major findings

Using nano-sized iron particles (having an average diameter of 2000 nm) mixed with a Prussian blue solution for staining iron, we demonstrated putative images of the EMFs emanating from the DP area of the human hair. Specifically, iron particle aggregates outlined the

Figure 5. Demonstration of EMFs triggering crystallization. Magnet fragment in SSP PBSFe2000 dry field, showing the orderly EMFs emanating from a non-living magnetic source. Although the inanimate magnetized object triggered crystallization there was an absence of heavy crystals adhering to the tip of the magnet (arrow). Also note that the further the distance from the magnetic source the wider the gap between the curved crystallization lines (see Supplementary Video 1).

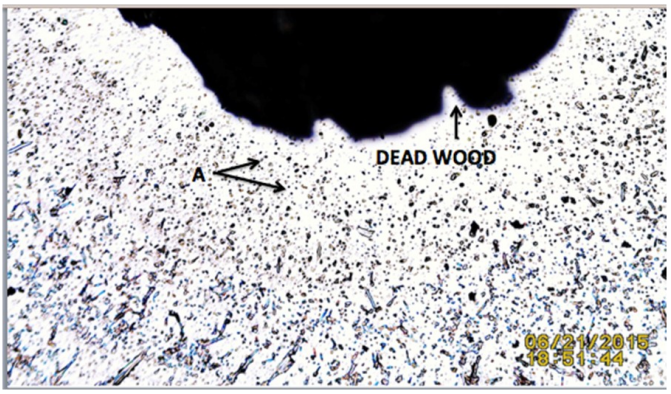

Figure 6. A SSP of a dead wood fragment (toothpick) in PBSFe2000, as a negative control. A depicts iron particles. Notice that an inanimate (dead) material is unable to trigger large crystals formation. This is attributed to the absence of EMFs (see Supplementary Video 2).

anatomical areas where S100 proteins have been located.

Background

A metabolic process common in animals (cellular respiration) involves the electron transport chain. This process consists of electrons transferred along a series of electron donor and receptor compounds coupled to a proton (H^+) gradient across cell membranes. The ensuing charge differential or voltage is used to drive energy production in the form of adenosine triphosphate (ATP). As inferred by Faraday's law, electron movement within cells will induce an electromagnetic field (EMF) emanating from both plant (Scherlag *et al.* 2015) and animal tissues (Embi *et al.* 2015a, b), acting as electrical conductors.

S100 proteins are only expressed in vertebrates. They consist of multiple constituents, which have both intracellular as well as extracellular functions. Furthermore, S100 are involved in aspects of regulation and energy metabolism. Those functions range from energy metabolism to cell proliferation, among others. In regard to energy metabolism, we hypothesize that the follicular metabolism is not only the source of electromagnetic energy but also free electrons, i.e. photoelectrons, which emanate from the follicle and can be tracked by the paramagnetic nano-sized iron particles.

Since our simple approach using nano-sized iron particles mixed with Prussian Blue Stain detects EMFs, is relatively inexpensive and provides an acute procedure, i.e., crystallization within <2 hours, it could easily be extended to various types of cellular research with minimal investment. For example, the S100 protein family has been reported to be present in multiple stages of tumorigenesis and cancer progression (Bresnick *et al.* 2015). Further research, using the methodology described in the present report, might be useful in evaluating chemotherapeutic drug effects by EMFs changes shown by cells and tissues.

Conclusion

Our results link the molecular biochemical energy associated with the S100 family of proteins and biomagnetism.

References

Baule GM & McFee R 1963 Detection of the magnetic field of the heart. *American Heart Journal* **66** 95-96

Bresnick AR, Weber DJ & Zimmer DB 2015 S100 proteins in cancer. *Nat Rev Cancer* **15** 96-109

Cohen D 1972 Magnetoencephalography: Detection of the Brain's electrical activity with a superconducting magnetometer. *Science* **175** 664-666

Cohen D & Kaufman LA 1975 Magnetic determination of the relationship between the ST segment shift and the injury current produced by coronary occlusion. *Circ Res* **36** 414-424

Cohen D, Savard P, Rifkin RD, Lepeshkin E & Strauss WE 1983 Magnetic measurement of S-T and T-Q segment shifts in humans. Part II; Exercise-induced S-T segment depression. *Circ Res* **53** 274-279

Donato R, Cannon BR, Sorci G, Riuzzi F, Hsu K, Weber DJ & Geczy CL 2013 Functions of S100 proteins. *Curr Mol Med.* **13** 24-57

Embi AA, Jacobson JI, Sahoo K & Scherlag BJ 2015a Demonstration of Inherent Electromagnetic Energy Emanating from Isolated Human Hairs. *Journal of Nature and Science* **1** e55

Embi AA, Jacobson Jl, Sahoo K & Scherlag BJ 2015b Demonstration of Electromagnetic Energy Emanating from Isolated Rodent Whiskers and the Response to Intermittent Vibrations. *Journal of Nature and Science* **1** e52

Mitoma C, Kohda F, Mizote Y, Miake A, Ijichi A, Kawahara S, Kohno M, Sonoyama H, Mitamura Y, Kaku Y, Inoue H, Sasaki Y, Ohno F, Okabe N, Take N, Mizote M, Masuda A & Furue M 2014 Localization of S100A2, S100A4, S100A6, S100A7, and S100P in the human hair follicle. *Fukuoka Igaku Zasshi* **105** 148 -156

Scherlag BJ, Huang B, Zhang L, Sahoo K, Towner R, Smith N, Embi AA & Po SS 2015 Imaging the electromagnetic field of plants (Vigna radiata) using iron particles: Qualitative and quantitative correlates. *Journal of Nature and Science* **1** e61